11-2-2010

Thermoelectric power investigations of YbAgGe across the quantum critical point

Eundeok Mun
Iowa State University, richflavor@gmail.com

Sergey L. Bud'ko
Iowa State University, budko@ameslab.gov

Paul C. Canfield
Iowa State University, canfield@ameslab.gov

Thermoelectric power investigations of YbAgGe across the quantum critical point

Abstract
The magnetic field and temperature dependences of the thermoelectric power (TEP) of the antiferromagnetically ordered heavy fermion compound YbAgGe are measured across the field-induced quantum critical point. These TEP measurements reproduce the earlier H-T phase diagram and identify an additional domelike phase between ~45and ~70 kOe. On the low-field side of this region, H>Hc~45 kOe, the sign of the TEP changes from negative to positive; on the high-field side of this region, H≈70 kOe, a non-Fermi-liquid state is evidenced as the logarithmic temperature dependence of S(T)/T, in agreement with previous specific heat results C(T)/T∝−log(T). For higher fields, H>70 kOe, the observed large value of α, S(T)=αT, is indicative of the heavy fermion state and shows a correlation with C(T)/T.

Keywords
Physics and Astronomy

Disciplines
Condensed Matter Physics

Comments
This article is from *Physical Review B* 82 (2010): 174403, doi:10.1103/PhysRevB.82.174403.

PHYSICAL REVIEW B **82**, 174403 (2010)

Thermoelectric power investigations of YbAgGe across the quantum critical point

Eundeok Mun, Sergey L. Bud'ko, and Paul C. Canfield
Ames Laboratory, US DOE and Department of Physics and Astronomy, Iowa State University, Ames, Iowa 50011, USA
(Received 22 July 2010; published 2 November 2010)

The magnetic field and temperature dependences of the thermoelectric power (TEP) of the antiferromagnetically ordered heavy fermion compound YbAgGe are measured across the field-induced quantum critical point. These TEP measurements reproduce the earlier H-T phase diagram and identify an additional domelike phase between ~45 and ~70 kOe. On the low-field side of this region, $H > H_c \sim 45$ kOe, the sign of the TEP changes from negative to positive; on the high-field side of this region, $H \approx 70$ kOe, a non-Fermi-liquid state is evidenced as the logarithmic temperature dependence of $S(T)/T$, in agreement with previous specific heat results $C(T)/T \propto -\log(T)$. For higher fields, $H > 70$ kOe, the observed large value of α, $S(T) = \alpha T$, is indicative of the heavy fermion state and shows a correlation with $C(T)/T$.

DOI: 10.1103/PhysRevB.82.174403 PACS number(s): 72.15.Jf, 75.20.Hr, 75.30.Mb, 75.30.Kz

I. INTRODUCTION

Intensive study of strongly correlated electronic systems (SCESs) has revealed the existence of quantum phase transitions from ordered states to disordered states driven by nonthermal control parameters such as chemical doping, pressure, and magnetic field.[1] In the quantum critical regime, these systems can manifest non-Fermi-liquid (nFL) behavior: the exponent of electrical resistivity, $\Delta\rho = AT^n$, has $n < 2$ and the electronic specific heat coefficient, $\gamma = C(T)/T|_{T\to 0}$, is either singular, so the effective mass diverges in the zero temperature limit, $C(T)/T \propto -\log(T)$, or has a nonanalytic dependence on temperature, so the effective mass is finite $C(T)/T \propto -\sqrt{T}$.[2] Among SCES, nFL behavior near a quantum critical point (QCP) has explicitly been identified for heavy fermion (HF) metals such as $CeCu_{6-x}Au_x$ (Ref. 3) which becomes magnetic when the Au atom is replaced Cu site ($x \sim 0.1$); $CePd_2Si_2$ (Ref. 4) in which the Néel temperature, T_N, is suppressed and superconductivity is induced by applying pressure; and $YbRh_2Si_2$ (Ref. 5) and YbAgGe (Ref. 6) both of which have antiferromagnetic (AFM) order which is suppressed by the application of an external magnetic field. When the system is tuned away from (beyond) the QCP, resistivity and specific heat indicate a recovery of the FL state.

Systematic thermodynamic and transport measurements of YbAgGe have shown that the behavior of this compound in the vicinity of the QCP differs from that of other examples of field-induced quantum criticality. The hexagonal HF metal YbAgGe, with a Kondo temperature of $T_K \sim 25$ K, orders antiferromagnetically below ~1 K.[6,7] The H-T phase diagram of YbAgGe for $\mathbf{H} \| \mathbf{ab}$ is shown in Fig. 1, constructed from the electrical resistivity $[\rho(T,H)]$,[6,8] magnetizaion $[M(T,H)]$,[9] specific heat $[C_p(T)]$,[6,9] and Hall resistivity $[\rho_H(T,H)]$ (Refs. 10 and 11) measurements. Thermodynamic and transport measurements show that there is a first order transition below 0.6 K in zero field[6,9,12] as well as either AFM order below 0.8–1 K or a crossover region between 0.6–1 K. The AFM order can be suppressed by applying magnetic field of $H_c \geq 45$ kOe. Inside the AFM state, for $H < H_c$, there are three different regions. The first order phase boundary of region I is clearly evidenced from $\rho(T,H)$ and $M(T,H)$ with hysteresis. The lower-field side of the phase boundary of region III was inferred primarily from $\rho(H)$ measurements whereas the top and higher-field side of the phase boundary are observable in all thermodynamic and transport measurements, without any detectable hysteresis. The top boundary of region II, denoted by the dotted line, has been inferred from broad features in $C_p(T)$ and $\rho(T)$ measurements. However, as magnetic field increases this top boundary evolves into clear, sharp features that form the high-field side of region III.

The crossover lines, T_{Hall} and T^*, were inferred from the slope changes in $\rho_H(H)$ data[10,11] and supported by features in $M(T,H)$ and $C_p(T)$ (Ref. 9) data. A detailed power law analysis of $\rho(T)$,[8] $\rho(T) = \rho_0 + AT^n$, results that the exponent $n = 1$ for $45 \lesssim H \lesssim 70$ kOe (region IV in Fig. 1), the exponent n gradually increases from 1 to 2 for $70 \lesssim H \lesssim 100$ kOe, and ultimately the FL region, denoted by the T_{FL} line in Fig. 1, emerges for $H > 100$ kOe, satisfying $\Delta\rho = AT^2$.[8] Note for $\mathbf{H} \| \mathbf{c}$ that the AFM order can also be suppressed for $H \sim 90$ kOe and FL state is recovered for $H > 150$ kOe.[6,8,11]

When a QCP is approached, either by varying temperature or magnetic field, from the FL state, a strong nFL signatures were observed; $\Delta\rho(T) = AT$ in region IV and $C(T)/T \propto -\log(T)$ is clearly found for $H \simeq 80$ kOe. The magnetic structure has been identified from the neutron scattering experiments;[13–15] in zero field the magnetic structure described by a commensurate propagation vector $\mathbf{k}_1 = (1/3, 0, 1/3)$,[13] in region II the magnetic structure changes to incommensurate with $\mathbf{k}_2 = (0, 0, 0.324)$,[14] and in region III the magnetic structure, with small staggered moment, is similar to that in region I,[15] with the small ordered moment between 0.15 and 0.4 μ_B per Yb ion.

In this paper, we report the thermoelectric power (TEP) measurements on YbAgGe. Systematic measurements of the TEP throughout the H-T phase space of a field-induced QCP have been limited to few cases in particular $YbRh_2Si_2$ (Ref. 16) and $CeCoIn_5$.[17] In order to clarify the anisotropic TEP response, measurements of TEP in this work were performed with two different heat-current directions.

II. EXPERIMENTAL

The single crystalline samples of YbAgGe were grown from a high temperature, ternary solution as outlined in Ref.

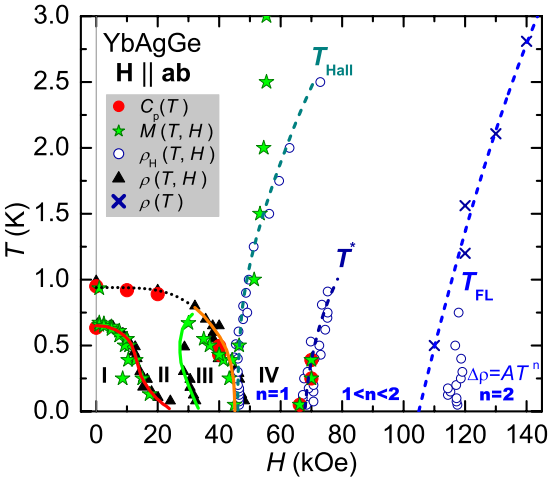

FIG. 1. (Color online) H-T phase diagram of YbAgGe for $\mathbf{H}\|\mathbf{ab}$, constructed from the specific heat $C_p(T)$ (Refs. 6 and 9), magnetizaion $M(T,H)$ (Ref. 9), Hall resistivity $\rho_H(T,H)$ (Ref. 11), and resistivity $\rho(T,H)$ (Refs. 6 and 8) measurements. Thick solid and dotted lines represent the magnetic phase boundaries. Dashed lines T_{Hall} and T^* are the crossover lines determined from the thermodynamic and transport measurements. The Fermi-liquid region denoted by the dashed, T_{FL} crossover line was determined from the region satisfying $\Delta\rho=AT^2$. See text for details.

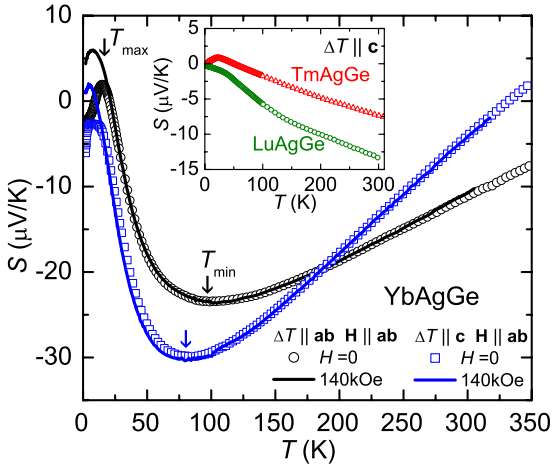

FIG. 2. (Color online) $S(T)$ of YbAgGe for $\Delta T\|\mathbf{ab}$ and $\Delta T\|\mathbf{c}$ at $H=0$ (symbols) and 140 kOe (lines), applied along hexagonal **ab** plane ($\mathbf{H}\|\mathbf{ab}$) in a transverse configuration, $\mathbf{H}\perp\Delta T$, for both heat flow directions. Arrows indicate the local minimum (T_{min}) and maximum (T_{max}) temperature. Inset: $S(T)$ of LuAgGe and TmAgGe at $H=0$.

18. The TEP was measured using a dc, alternating heating, technique utilizing two heaters, and two thermometers.[19] This specially designed setup was used in a Quantum Design Physical Property Measurement System over the temperature range from 2 to 350 K and magnetic fields up to 140 kOe, and in a CRYO Industries of America ^{3}He system from 0.3 to 30 K and up to 90 kOe. Single crystals of YbAgGe were cut using a wire-saw and then polished down to the desired dimensions of $\sim 0.2\times 0.15\times 3$ mm^3. The needle-shaped samples were directly attached to the two Cernox thermometers using DuPont 4929N silver paint.[19] Note that the TEP value of the lead wire (phosphor-bronze) is ignored since the TEP of this wire is negligible.[19] The anisotropic TEP measurements were performed with two different heat-current directions, generated in the hexagonal **ab** plane and along the **c** axis, and the temperature difference (ΔT) along the samples was kept between 0.03–0.05 K below 2 K. The magnetic field was applied in the **ab** plane for both ΔT directions maintaining a transverse configuration, $(\mathbf{H}\|\mathbf{ab})\perp(\Delta T\|\mathbf{ab})$ and $(\mathbf{H}\|\mathbf{ab})\perp(\Delta T\|\mathbf{c})$, in both cases.

III. RESULTS

The temperature-dependent TEP, $S(T)$, of YbAgGe for both $\Delta T\|\mathbf{ab}$ and $\Delta T\|\mathbf{c}$ measured for $H=0$ and 140 kOe are plotted in Fig. 2; for comparison $S(T)$ data for isostructural LuAgGe and TmAgGe are displayed in the inset. The $S(T)$ plot for LuAgGe is typical of those found in normal metals, consistent with resistivity and Hall coefficient measurements.[10,18] At high temperatures, the absolute value of TEP for TmAgGe is smaller than that of LuAgGe, however the slope, $dS(T)/dT$, is similar for both compounds. In contrast to LuAgGe, the $S(T)$ data of TmAgGe manifest a broad peak around 25 K, followed (upon warming) by sign change from positive to negative at 53 K.

For YbAgGe, above 25 K, a qualitatively similar temperature dependence for both ΔT directions is seen for $S(T)$ in zero and high magnetic field, which is negative and reveals a broad local minimum around $T_{min}\sim 85$ K with the TEP values between -20 and -30 μV/K, typical of those found in other Yb-based, Kondo lattice systems.[20] At low temperatures the observed $S(T)$ is anisotropic; in zero field, $S(T)$ for $\Delta T\|\mathbf{c}$ remains negative over the whole temperature range measured, whereas $S(T)$ for $\Delta T\|\mathbf{ab}$ manifests sign reversals at $T_{SR}=21$ and 9.5 K. Sign changes at similar temperatures have been observed in ρ_H measurements.[10,11]

Figures 3(a) and 3(b) show the low temperature $S(T)$ for $\Delta T\|\mathbf{ab}$ and $\Delta T\|\mathbf{c}$, respectively, in selected fields. In zero field the observed $S(T)$ data manifest rich and complex structures involving sign reversals, T_{SR} (not marked in Fig. 3), a clear maximum centered at $T_{max}\sim 15$ K, a gradually decreasing TEP followed by plateau region (T_0), followed at lower temperature by a sharp drop, and finally a weak slope change and an abrupt change associated with the long range magnetic order $T_N\sim 0.8$ K and $T_{N1}\sim 0.65$ K, respectively. As magnetic field increases, $S(T)$ reveals systematic changes in these anomalies: T_N, T_{N1}, T_{max}, and T_{SR}. The evolution of these features with magnetic field will be discussed in detail below. Similar features are apparent in the $\Delta T\|\mathbf{ab}$ and $\Delta T\|\mathbf{c}$ data sets. The biggest difference is that a clear positive peak at T_{max} develops for $\Delta T\|\mathbf{ab}$ whereas a shoulder occurs for $\Delta T\|\mathbf{c}$.

Below T_{max}, an inflection point around $T_0\sim 5$ K, determined as the local maximum in $dS(T)/dT$, is observed in zero field for both ΔT directions. This characteristic temperature is also evident in the bulk magnetic susceptibility which shows a broad peak around 5 K along $\mathbf{H}\|\mathbf{ab}$.[18] Neutron scattering experiments[13] show that the characteristic energy scale $\Gamma_\mathbf{q}$ at the AFM zone boundary has a discontinuity at $T\sim 5$ K. Whereas $\Gamma_\mathbf{q}$ at the AFM zone center increases rap-

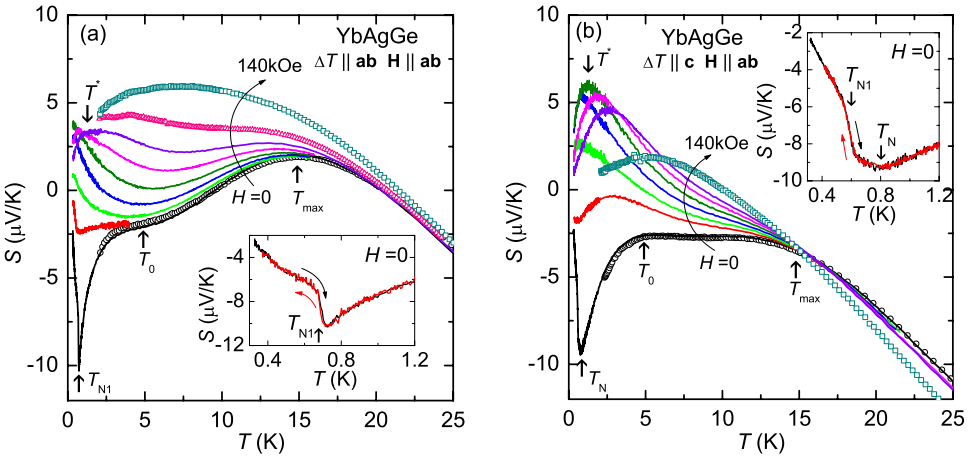

FIG. 3. (Color online) Low-temperature $S(T)$ of YbAgGe for $\Delta T \| \mathbf{ab}$ (a) and $\Delta T \| \mathbf{c}$ (b) in selected fields, $H=0$, 40, 50, 60, 70, 80, 90, 110 (only for $\Delta T \| \mathbf{ab}$), 140 kOe (bottom to top), applied along the **ab** plane in a transverse configuration ($\mathbf{H} \perp \Delta T$) for both heat flow directions. Symbols and lines are taken from ^{4}He and ^{3}He measurement setup, respectively. The local maximum temperature $T_{\max}$, inflection point T_0, magnetic order T_N and T_{N1}, and field-induced local maximum T^* are marked by arrows. Inset: (a) low-temperature $S(T)$ for $\Delta T \| \mathbf{ab}$ at $H=0$, taken data both warming up and cooling down the temperature. Arrow indicates the phase transition temperature T_{N1}. Inset: (b) low-temperature $S(T)$ for $\Delta T \| \mathbf{c}$ at $H=0$, taken data both warming up and cooling down the temperature. Arrows indicate the phase transition temperature T_{N1} and the local minimum temperature corresponding to T_N.

idly without any discontinuity as temperature increases, following $\sqrt{T}$ behavior usually shown in HF compounds such as $CuCu_6$.[21] This particular **q** dependence of the strong antiferromagnetic spin fluctuations, may be a responsible for anisotropic TEP at low temperature, as well as the inflection at temperature T_0. Anisotropic TEP may also be related to the different scattering rates due to the anisotropic Fermi surface.

For $H>70$ kOe the development of local maximum at T^* can be clearly seen in $S(T)$ for both ΔT directions, although it more clearly develops for $\Delta T \| \mathbf{c}$ than for $\Delta T \| \mathbf{ab}$. This maximum shifts to higher temperature as magnetic field increases. At least up to 90 kOe it seems to be clear that $T_{\max}$ is magnetic field independent and T^* is approximately proportional to the magnetic field. At higher fields, above 110 kOe, these two peaks merge into one peak structure. Note that a similar development of such a peak structure has also been observed in specific heat measurements in the similar temperature and magnetic field regime.[6,9]

As was suggested in earlier studies, YbAgGe shows a broad feature at $T_N \sim 0.8-1$ K and a sharp, first order phase transition at $T_{N1} \sim 0.65$ K which manifests clear hysteresis in resistivity and magnetization measurements.[8,9] As shown in the inset of Fig. 3(a) in zero field the $S(T)$ data for $\Delta T \| \mathbf{ab}$ show a sharp jump below ~ 0.7 K (T_{N1}) without hysteresis within our measurement resolution ($\Delta T \sim 30$ mK). For $\Delta T \| \mathbf{c}$ [inset of Fig. 3(b)] a broad local minimum is located near $T_N \sim 0.8$ K and a sharp jump upward occurs at $T_{N1} \sim 0.6$ K. When magnetic field is applied, the shape of the anomaly at T_{N1} broadens and develops a clear hysteresis as it shifts to lower temperatures (see Fig. 4 below). The isomagnetic field [$S(T)$] and isothermal [$S(H)$] data can be used to establish a H-T phase diagram. The TEP response to a magnetic phase transition has not been well established and, in the case of AFM compounds, sometimes TEP shows no clear indication of the phase transition.[16,22] Hence, we present all $S(T)$ data for $\Delta T \| \mathbf{ab}$ in Fig. 4 and outline the criteria we have established for tracking transitions.

As shown in Fig. 4(a), a sudden jump at T_{N1} is clearly seen for $H<15$ kOe, that corresponds to the boundary of region I in Fig. 1. Initially, the data were taken upon warming from the base temperature to $T>1.5$ K and then the data were collected upon cooling down to base temperature, allowing for evaluation of hysteresis. The critical temperature for this phase line was determined from the minimum of $dS(T)/dT$. The T_{N1} in zero field is suppressed to lower temperature and the hysteresis becomes significant as magnetic field increases. Note that a very large splitting between warming and cooling curves below ~ 0.5 K is observed for $H=12.5$ kOe and a broad local minimum near 0.6 K begins to develop. The determined phase transition temperatures are plotted below in Fig. 8 as solid up-triangles for warming and solid down-triangles for cooling. As magnetic field increases (region II) the abrupt jump in $S(T)$ changes to a broad local minimum first seen for $H=12.5$ kOe [arrow in Fig. 4(a)] and seen evolving in Fig. 4(b). In this plot, only the data taken upon warming are plotted because no detectable hysteresis was observed for $H \geq 15$ kOe, for example, as seen for $H=15$ kOe curves in Fig. 4(a). It is not clear at present whether this minimum is a phase transition or a crossover. This minimum is denoted by solid circles in Fig. 8 below. At $H=25$ kOe two slope changes are observed near 0.6 and 0.75 K. For higher fields, $25<H<45$ kOe [Fig. 4(c)], the broad minimum in region II becomes sharp and the slope change shifts to lower temperature with increasing magnetic field. This sharp slope change is indicated by arrows in Fig. 4(c) and plotted in Fig. 8 (below) as solid squares.

For still higher fields, $45<H<70$ kOe [Fig. 4(d)], there is a weak slope change below 0.6 K. The slope change is most clearly seen in the $H=55$ kOe data and is indicated by arrows in Fig. 4(d), and is represented in Fig. 8 (below) as stars. Note for $H=70$ kOe data, $S(T)$ increases linearly as

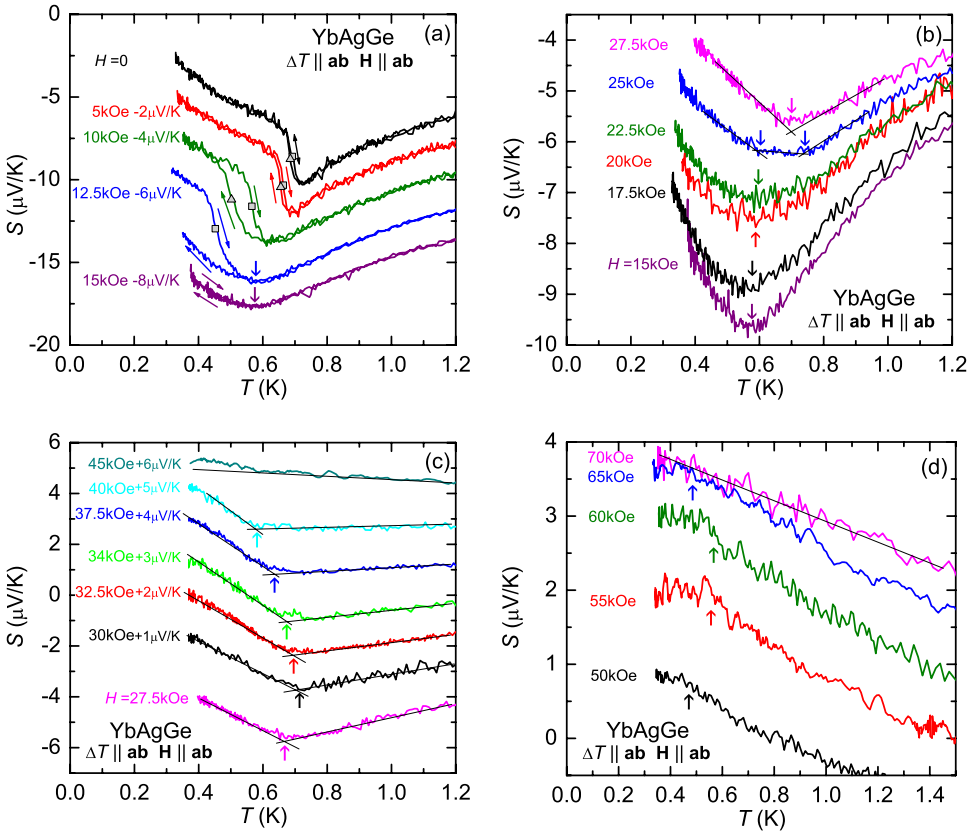

FIG. 4. (Color online) Low-temperature $S(T)$ of YbAgGe for $\mathbf{H}\|\mathbf{ab}$ and $\Delta T\|\mathbf{ab}$ ($\mathbf{H}\perp\Delta T$). $S(T)$ curves in (a), (b), (c), and (d) correspond to the region I, II, III, and IV in Fig. 1, respectively. $S(T)$ curves in (a) and (c) are shifted for clarity. (a) Squares and triangle symbols indicate phase transition temperatures determined from $dS(T)/dT$ and the arrows represent the local minimum. The data, taken for both warming and cooling the temperature, are plotted. Arrows in (b), (c), and (d) indicate the local minimum and slope change. The data are presented only taken upon warming the temperature. Solid lines are guide to the eyes. See text for details.

temperature decreases without any slope change below 1.5 K. In this field regime, no clear feature of a phase transition has been detected in any of the earlier studies.[6,8,9,11] However, a broad feature occurs in the magnetization and specific heat data.[9] For further increasing magnetic field ($H>70$ kOe) a local maximum T^* develops as shown in Fig. 3(a). The position of T^* was determined from a Gaussian curve fit to the $S(T)$ data and plotted in Fig. 8 (below) as the cross symbols.

One of the most striking features of the $S(T)$ measurements is the different manifestations of the magnetic phase transitions for the two different directions of heat flow. When the AFM ordering takes place, $S(T)$ for $\Delta T\|\mathbf{c}$ manifests a broad minimum at $\sim$0.8 K which is close to the temperature identified as T_N from earlier studies of $C_p(T)$, $\rho(T)$, and $M(T)$ (Refs. 6 and 9) and an abrupt jump without measurable hysteresis at $T_{N1}\sim$0.6 K as shown in the inset of Fig. 3(b). As magnetic field increases (Fig. 5), T_N shifts to lower temperature and it is completely suppressed for $H>50$ kOe whereas the feature identified as T_{N1} fades away very rapidly and is not detected for $H>10$ kOe. The evolution of T_N with varying magnetic field are shown in Fig. 5, where the arrows are determined from $dS(T)/dT$ (inset, Fig. 5). These phase boundaries are plotted in Fig. 8 as open up-triangles for T_N and open circle for T_{N1}. Note for the $H=40$ kOe curve that the local minimum at this magnetic field is not discernible, instead $S(T)$ flattens below $\sim$0.6 K.

Figures 6(a) and 6(b) show the field-dependent TEP, $S(H)$, at selected temperatures. $S(H)$ measurements provide orthogonal cuts through the H-T phase diagram (Fig. 1) and shed further light on some of the features observed in $S(T)$.

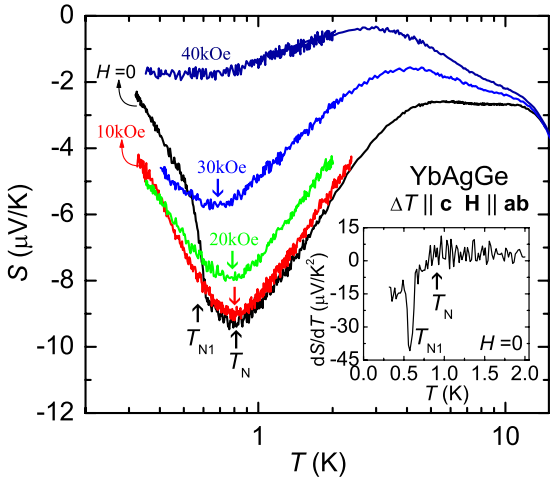

FIG. 5. (Color online) Low-temperature $S(T)$ of YbAgGe for $\mathbf{H}\|\mathbf{ab}$ and $\Delta T\|\mathbf{c}$. In zero field up-arrows indicate the abrupt jump (T_{N1}) and local minimum (T_N), respectively, determined from $dS(T)/dT$ (inset). Down-arrows indicate the local minimum temperatures corresponding to the T_N. Inset: $dS(T)/dT$ at $H=0$.

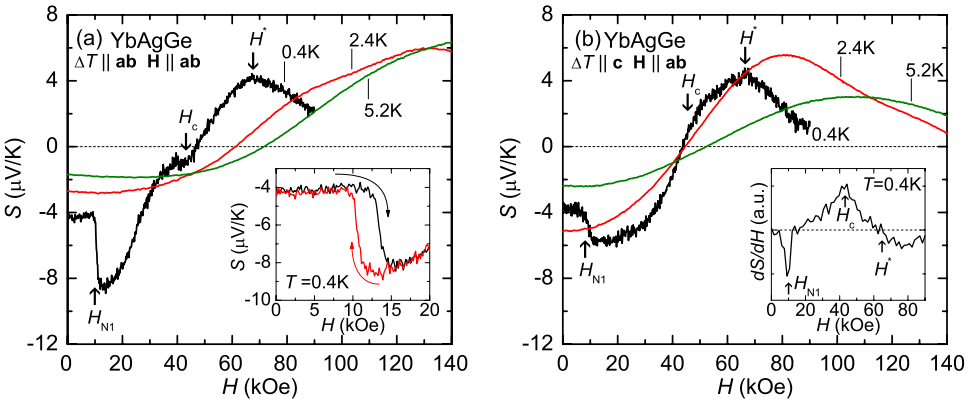

FIG. 6. (Color online) $S(H)$ of YbAgGe for $\Delta T \| \mathbf{ab}$ (a) and $\Delta T \| \mathbf{c}$ (b) at selected temperatures of 0.4, 2.4, and 5.2 K, and for magnetic field applied along $\mathbf{H} \| \mathbf{ab}$ in a transverse configuration ($\mathbf{H} \perp \Delta T$). Arrows indicate phase transitions (H_c and H_{N1}) and local maximum field (H^*), determined from $dS(H)/dH$. Inset: (a) $S(H)$ for $\Delta T \| \mathbf{ab}$ at 0.4 K, taken data with both increasing and decreasing magnetic field. (b) $dS(H)/dH$ for $\Delta T \| \mathbf{c}$ at 0.4 K.

For $\Delta T \| \mathbf{ab}$ at $T=0.4$ K [Fig. 6(a)], $S(H)$ data show a sudden jump at $H_{N1}=13$ kOe which is hysteretic (inset) and a slope change around $H_c=42$ kOe. In addition, a broad maximum appears at $H^* \sim 68$ kOe. Note that H_{N1}, H_c, and H^* were determined from $dS(H)/dH$ analysis by a sharp peak, slope change (or minimum), and $dS(H)/dH=0$, respectively. Although an anisotropic response of $S(H)$ to the magnetic field is observed for the two different directions of heat flow, the characteristic magnetic fields for the long range magnetic order and the crossover field H^* remain qualitatively the same for both ΔT directions: for $\Delta T \| \mathbf{c}$ at $T=0.4$ K shown in Fig. 6(b), $S(H)$ data show distinct features at ~ 10 kOe and ~ 67 kOe corresponding to H_{N1} and H^* for $\Delta T \| \mathbf{ab}$, respectively. A very weak slope change around 42 kOe corresponding to H_c for $\Delta T \| \mathbf{ab}$ is also observed, where the derivative $dS(H)/dH$ (inset) clearly shows a slope change (or maximum) around 42 kOe. The phase transition fields, H_{N1} and H_c, for $\Delta T \| \mathbf{c}$ are represented by open triangles ($\triangleright$) in Fig. 8. Note that the lower-field boundary of region III in Fig. 1 was not observed in TEP measurements for either ΔT direction, where $S(H)$ varies without any kink or significant slope change from 15 to 40 kOe. For $\Delta T \| \mathbf{c}$, the H^* evolve in basically the same way as for $\Delta T \| \mathbf{ab}$. Note that $S(H)$ for $\Delta T \| \mathbf{c}$ shows an additional broad feature near ~ 90 kOe for $T=2.4$ K curve.

The evolution of H_{N1}, H_c, and H^* for $\Delta T \| \mathbf{ab}$ is shown in Figs. 7(a) and 7(b). As temperature increases H_{N1} and H_c shift to lower magnetic fields and H^* moves to higher magnetic fields. The arrows, $\leftarrow$, $\downarrow$, and $\uparrow$, are represented by symbols, $\blacktriangleright$, $\blacklozenge$, and +, respectively, in Fig. 8. When the temperature is lowered, the hysteresis at H_{N1} is more pronounced as shown in the inset of Fig. 7(a).

Since TEP in zero field manifests a sign reversal at low temperatures and the possibility of a sign reversal at the QCP has been proposed,[23] it is of interest to see the evolution of the TEP sign change as the system is tuned by magnetic field [Fig. 7(a)]. For $\Delta T \| \mathbf{ab}$ the negative TEP sign in zero field changes to positive for $H_{SR} > 47$ kOe at 0.4 K. The H_{SR} at 0.4 K shifts to higher fields as temperature increases, indicated by the large, open arrows in Fig. 7(a). The sign reversal temperatures obtained from $S(T,H)$ measurements for $\Delta T \| \mathbf{ab}$ are plotted in Fig. 8 as $\times$ symbols. Note that the sign

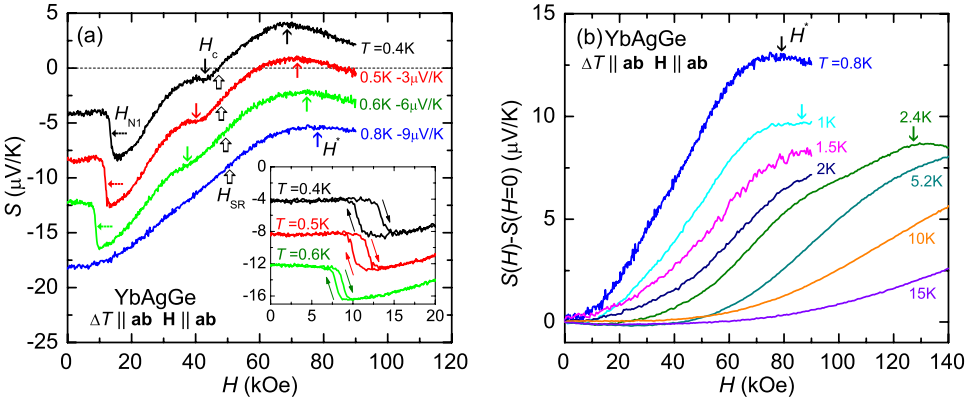

FIG. 7. (Color online) $S(H)$ of YbAgGe for $\Delta T \| \mathbf{ab}$ and for magnetic field applied along $\mathbf{H} \| \mathbf{ab}$ in a transverse configuration ($\mathbf{H} \perp \Delta T$). (a) $S(H)$ at 0.4, 0.5, 0.6, and 0.8 K, taken data with increasing magnetic field. Curves for $T=0.5$, 0.6, and 0.8 K are shifted for clarity. Arrows indicate phase transitions $H_{N1}(\leftarrow)$ and H_c ($\downarrow$), a sign reversal ($\Uparrow$), and a local maximums H^* ($\uparrow$). Inset: hysteresis curves of $S(H)$ measurements at $T=0.4$, 0.5, and 0.6 K. (b) Normalized TEP $[S(H)-S(H=0)]$ as a function of H at $T=0.8$, 1, 1.5, 2, 2.4, 5.2, 10, and 15 K. Arrows indicate a local maximum H^*.

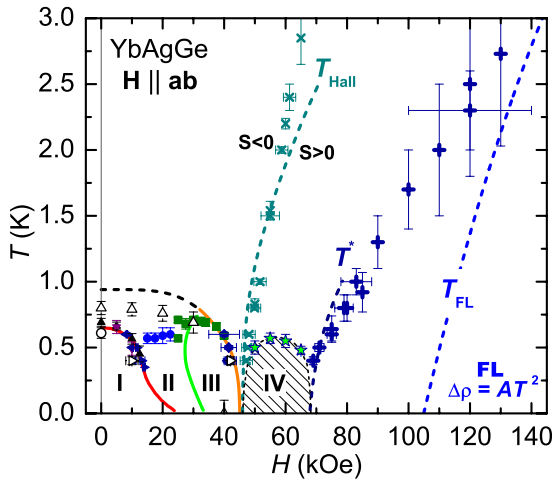

FIG. 8. (Color online) H-T phase diagram of YbAgGe for $\mathbf{H}\|\mathbf{ab}$. Solid symbols are inferred from $\Delta T\|\mathbf{ab}$ data and open symbols are inferred from $\Delta T\|\mathbf{c}$ data, plotted on the top of phase and crossover lines in Fig. 1; ▲ (△,○) from up-sweeps in T, ▼ from down-sweeps in T, ▶ (▷) from up-sweeps in H, ◀ from down-sweeps in H, and other symbols (●, ■, ◆, ★, ×, +) from up-sweeps in T and H. The × symbols indicate the sign reversal on TEP from negative to positive. The + symbols correspond to the local maximum developed in $S(T,H)$. The FL region was taken from earlier $\rho(T)$ ($\Delta\rho=AT^2$) measurements (Refs. 6 and 8).

reversal of TEP for $\Delta T\|\mathbf{c}$ is essentially similar to that for $\Delta T\|\mathbf{ab}$ below 2 K. At 0.4 K the TEP sign for $\Delta T\|\mathbf{c}$ changes from negative to positive for $H>44$ kOe [Fig. 6(b)].

IV. DISCUSSION

At low temperatures, TEP measurements on YbAgGe indicate complex sign variations as temperature and magnetic field vary. For $\Delta T\|\mathbf{ab}$, in zero field [Fig. 3(a)] the sign reversal in $S(T)$ occurs at $T_{SR}=21$ and 9.5 K. As magnetic field increases T_{SR} shown at 21 K moves to slightly higher temperatures, T_{SR} at 9.5 K moves down and a third sign reversal occurs at lower temperatures: $H_{SR}=47$ kOe at 0.4 K [Fig. 7(a)]. For $\Delta T\|\mathbf{c}$, in zero field TEP remains negative for all $T<300$ K (Fig. 2), but, at low temperatures, it moves gradually to positive with increasing magnetic field, becoming positive for $H_{SR}>44$ kOe at 0.4 K [Fig. 6(b)]. Similar behavior, but with opposite sign change, has been observed in ρ_H measurements.[10,11] As temperature decreases, the Hall coefficient, ρ_H/H, remains positive down to 50 mK for $\mathbf{H}\|\mathbf{ab}$ and the Hall voltage along (approximately) the $\mathbf{c}$ axis whereas a sign reversal from positive to negative is observed for $\mathbf{H}\|\mathbf{c}$ and the Hall voltage in the $\mathbf{ab}$ plane. At this stage it is difficult to explain low-temperature sign reversal for both $S(T)$ and ρ_H/H which may arise from the multisheet Fermi surface of electrons and holes with different mobilities. The conductivity change is mainly determined by the change in the electron velocity at the Fermi level and the sign of the derivative of density of states (DOS) does not depend on the sign of the velocity but depends on the curvature of the dispersion of quasi-particles.[24,25] This may explains the discrepancy of sign between TEP and Hall coefficients of YbAgGe; $S>0$ and $\rho_H/H<0$ at high temperatures. At low temperatures, an explanation of the complex sign reversal in the TEP is not simple because one should consider contribution from all bands with relevant weights of heavy and light carriers.

TEP is known to be particularly sensitive to Kondo (T_K) and crystalline electric field (CEF, Δ_{CEF}) effects, and to various physical quantities related to the DOS because of the energy-dependent formula at the Fermi level:[24] $S=-\frac{\pi^2 k_B^2 T}{3e}\left(\frac{\partial \ln\sigma(\varepsilon)}{\partial\varepsilon}\right)_{\varepsilon_F}$, where e is the elementary charge, ε_F is the Fermi energy, and $\sigma(\varepsilon)$ is the transport integral. Although TEP can probe various salient energy scales, the interpretation of its temperature and magnetic field dependence is often difficult, even for simple metals. Since a quantitative analysis of TEP is very difficult, we assumed that the present TEP data reflect the remaining $4f$ magnetic contribution of trivalent Yb ions, especially the position of the local extrema, the large absolute value, and the abrupt change associated with long range magnetic order.

The characteristic temperatures, $T_{\max}$ and $T_{\min}$, allow for the evaluation of T_K and Δ_{CEF} as relevant energy scales in YbAgGe. In zero field, $T_{\max}$ and $T_{\min}$, as shown in Fig. 2, can be related to Kondo scattering associated with the CEF ground state and the excited CEF multiplet levels, respectively. For HF Kondo lattice compounds, in general, it has been shown that the lower temperature maximum is close to T_K and the higher temperature minimum develops roughly within $0.3\Delta_{\mathrm{CEF}}-0.6\Delta_{\mathrm{CEF}}$, which is in agreement with theoretical predictions.[26–29] Inelastic neutron scattering experiments on YbAgGe have proposed the CEF level scheme with doublet levels located approximately at 0-140-230-330 K.[30] This scheme is consistent with the specific heat analysis (0-110-190-335 K) involving combined Kondo effect ($T_K=24$ K) and electronic Schottky contributions.[7] Thus, the doublet ground state and T_K are well separated from the first excited CEF level. From the TEP measurements shown in Fig. 2 an estimate of the energy-level splitting lies between 140 and 280 K with respect to the ground-state doublet. The lower end of this range, $T_{\min}\sim 0.6\Delta_{\mathrm{CEF}}$, is very close to the value obtained in the inelastic neutron scattering and specific heat analysis. Thus, we conclude that $T_{\min}$ with the large, negative, absolute value can be attributed to Kondo scattering on an excited CEF multiplet of Yb^{3+}.

In general a phonon-drag contribution to the TEP appears between $0.1\Theta_D-0.3\Theta_D$ with a broad peak structure,[24,31] where Θ_D is the Debye temperature. For YbAgGe with $\Theta_D\sim 300$ K,[18] $T_{\max}$ is far below the expected temperature due to the phonon drag. For comparison, the TEP plots of the isostructural compounds, LuAgGe and TmAgGe, do not manifest any conspicuous signatures of phonon drag either (inset of Fig. 2). LuAgGe has a slope change around 35 K ($\sim 0.12\Theta_D$), and TmAgGe, $S(T)$ shows a broad peak around 25 K expected due to either phonon drag or CEF splitting. The absolute TEP value of both compounds is small compared to that of YbAgGe and the temperatures of anomalies seen for both compounds are higher than $T_{\max}$ for YbAgGe. Therefore, we expect that the origin of $T_{\max}$ is not the phonon drag.

On the other hand, it seems reasonable that $T_{\max}$ is caused by the Kondo effect. In a number of HF compounds the

Kondo effect manifests itself as a maximum in $S(T)$ in the vicinity of the T_K.[32–34] In a similar way the resistivity curve of YbAgGe displays a characteristic behavior in which the resistivity decreases rapidly below ~100 K expected due to the CEF effect and shows a hump below 25 K related to the development of coherent quasi-particles.[18] We therefore assume that $T_{\max}$ in TEP measurements represents the crossover temperature (T_K) from local moment to HF behavior. A similar order of magnitude of T_K is also estimated from the specific heat and neutron scattering experiments. However, T_K obtained from TEP is smaller than the one obtained from the specific heat. Since T_K is not a phase transition temperature but a crossover, a different crossover temperature, but of similar order of magnitude, can be expected from different measurements.

Figure 8 shows the H-T phase diagram based on the TEP measurements. All data points inferred from $S(T)$ track well the data inferred from $S(H)$ data. The closed symbols are taken from $\Delta T \| \mathbf{ab}$ and open symbols are taken from $\Delta T \| \mathbf{c}$, respectively. The TEP data are plotted on the top of the lines from Fig. 1. The clear agreement between TEP data and earlier thermodynamic and transport results indicates that TEP measurements can be a useful tool to refine and extend the H-T phase diagram. The sign reversal ($\times$), shown for $45 < H < 65$ kOe, and local maximum (+), shown for $H > 70$ kOe, are taken from $\Delta T \| \mathbf{ab}$. The phase boundary of region I, showing the hysteresis from both $S(T)$ and $S(H)$ measurements, is consistent with earlier studies. The top of region II, reflected by a broad local minimum in $S(T)$, may not be a phase transition but a crossover, since any clear signature of the phase transition in this temperature and magnetic field region has not been observed from earlier thermodynamic and transport measurements. The top and higher field boundary of region III are clearly seen in both $S(T)$ and $S(H)$ data; this phase transition line tends to go toward zero for $H_c \sim 45$ kOe.

The upper boundary (T_N) of region I and II was determined from the local minimum in $S(T)$ for $\Delta T \| \mathbf{c}$ (Fig. 5). It is clear that no signature of the upper boundary is observed for $\Delta T \| \mathbf{ab}$, which is similar to resistivity results.[8] By contrast, the observed TEP for $\Delta T \| \mathbf{c}$ indicates both T_N and T_{N1} in zero field, which is very similar to the specific heat measurements.[6,9] As magnetic field increases, T_N shifts to lower temperature and seems to be suppressed for $H > 45$ kOe, merging together with the high magnetic field boundary of region III and the T_{Hall} crossover line.

In earlier versions of the YbAgGe (H-T) phase diagram[6,8–11] two well-separated crossover lines, T_{Hall} and T^*, were seen and the long range magnetic order was suppressed to zero at $H_c \simeq 45$ kOe. The T_{Hall} line is well matched with the sign reversal of the TEP and T^* follows the local maximum observed in $S(T,H)$ measurements (Fig. 8). The T^* shifts to higher temperature as magnetic field increases and the peak position roughly follows an anomaly shown in $C_p(T)$ measurements.[9] Importantly, upon decreasing temperature ($T \to 0$), the features associated with these crossover lines, obtained from all the thermodynamic and transport measurements, converge to the same magnetic field values of $H_c \sim 45$ kOe and $H^* \sim 70$ kOe. Hence, it is expected that, when $T \to 0$, the sign of TEP will change from negative to positive at ~45 kOe for both ΔT directions and a peak structure in $S(H)$ data will be developed at ~70 kOe since the feature at H^* sharpens as temperature decreases.

It has been observed that the TEP measurements of $YbRh_2Si_2$ with a longitudinal configuration ($\mathbf{H} \| \Delta T$) manifest a sign reversal across the field-induced QCP.[16] A recent theoretical work[23] proposed the possibility of such TEP sign reversal at the QCP and was applied to the $YbRh_2Si_2$. The sign reversal for $YbRh_2Si_2$ is present inside the AFM state and terminates at the critical field whereas the sign reversal for YbAgGe emerges at the critical field and persists up to high temperature. For $CeRu_2Si_2$,[35] the positive TEP in zero field also changes sign above the metamagnetic field for $\Delta T \| \mathbf{c}$. Therefore, it is suggestive that the sign reversal can be an additional tool to probe and identify a QCP. Clearly, further theoretical and experimental investigations of this issue are required.

In addition to reproducing the earlier phase diagram in regions I, II, and III, the TEP measurements also delineate a new region: IV. The high-temperature boundary of the domelike area, located between T_{Hall} and T^* crossover line (region IV, Fig. 8), was determined by a slope change in $S(T)$ [Fig. 4(d)]. In this region the temperature dependences and large absolute values of the TEP are significantly different from that expected for the normal metal. Thus, the observed TEP in region IV suggests an unconventional magnetic or electronic origin.

Between the T_{Hall} and T^* crossover lines hints of such a domelike region were seen as broad features in earlier $M(H)$ and $C_p(T)$ studies but not identified as a possible transition. For instance, upon increasing magnetic field, the magnetization divided by magnetic field, $M(H)/H$, shows a considerable decrease passing through this region.[9] More significantly, the power-law analysis of resistivity[8] indicates a strong nFL behavior, $\rho(T) \propto T$, in this domelike area, where the boundary of maximum temperatures satisfying $\Delta\rho \propto T$ coincides with the boundary of the region IV. Therefore, the detection of this newly identified, domelike region appears to be robust in YbAgGe. When the magnetic field increases from AFM (region III) to this region with $\rho(T) \propto T$ (region IV), the lower-field boundary of the domelike region manifests as sudden jump in $M(H)/H$ and $C(T)/T$, as a sharp peak in magnetostriction (λ_{ab}) (Ref. 36) and ρ_H/H, and as a sign change in $S(H)$, however the higher-field boundary of the domelike region manifests itself as a smooth evolution of $M(H)/H$, $C(T)/T$, λ_{ab}, and ρ_H/H and as a peak structure in $S(H)$. It is not clear at this point if the domelike region is a magnetic field induced metamagnetic phase or electronic-structure change (e.g., topology change of the Fermi surface). To clarify this mysterious region further microscopic measurements, such as neutron scattering experiments, will be needed.

It is worth noting that although this region has not been identified at ambient pressure, a similar region in the H-T phase diagram has been identified in recent pressure measurements.[37] At 0.95 GPa, region IV appears in the high magnetic field region between ~45 and ~65 kOe and with increasing pressure (1.5 and 2.2 GPa) a new phase region between ~65 and ~90 kOe also develops. This behavior in the H-T-P phase space has been associated with the partial

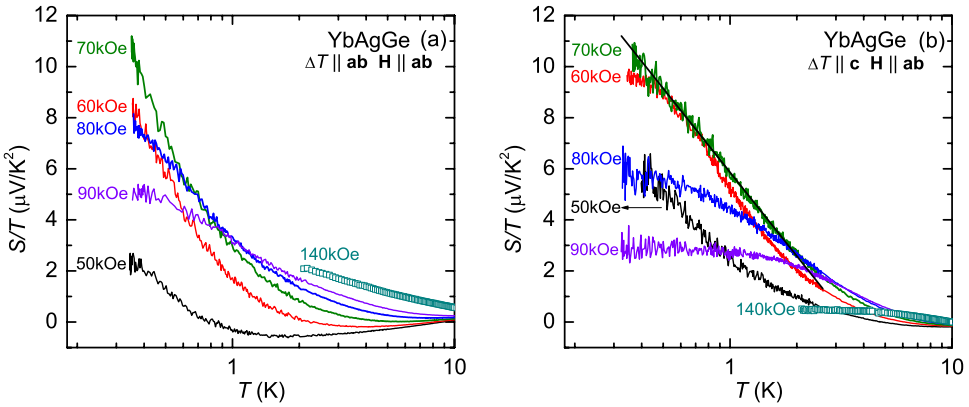

FIG. 9. (Color online) $S(T)/T$ of YbAgGe on a log(T) scale for both (a) $\Delta T \| \mathbf{ab}$ and (b) $\Delta T \| \mathbf{c}$ in selected magnetic fields, applied along $\mathbf{H} \| \mathbf{ab}$ in a transverse configuration ($\mathbf{H} \perp \Delta T$). Solid line in (b) on the top of 70 kOe data is a guide to the eyes.

release of the magnetic frustration in the quasi-kagome lattice of Yb ions under pressure.[37] Note that recently, a finite range of nFL behavior, separating FL region from AFM state, has been observed from Ge- and Ir-doped $YbRh_2Si_2$.[38,39]

Inside the domelike region IV, the TEP deviates from standard FL behavior, $S(T)=\alpha T$, where the observed $S(T)/T$ for both ΔT directions does not show a tendency of saturation at low temperatures. As shown in Fig. 9(a) for $\Delta T \| \mathbf{ab}$ and Fig. 9(b) for $\Delta T \| \mathbf{c}$, $S(T)/T$ increases inside region IV as magnetic field increases, reaching the maximum around 70 kOe, and then decrease with further increase in the magnetic field. It should be noticed that at $H=70$ kOe, $S(T)/T$ for $\Delta T \| \mathbf{c}$ manifests a clear, logarithmic temperature dependence as a signature of nFL behavior over about an order of magnitude in temperature. This is consistent with the specific heat results that also manifest $C(T)/T \propto -\log(T)$ at similar fields.[6] However, $S(T)/T$ for $\Delta T \| \mathbf{ab}$ increases more slowly than that for $\Delta T \| \mathbf{c}$ when temperature is lowered below 10 K. In order to clarify the existence of the logarithmic temperature dependence for $\Delta T \| \mathbf{ab}$ and to explore possibly of larger temperature range of such behavior, it is necessary to measure TEP below 0.3 K. Logarithmic temperature dependencies of specific heat and TEP in $YbRh_2Si_2$ (Ref. 16) and $CeCu_{6-x}Au_x$ (Ref. 40) has been observed in the vicinity of QCP, which are supported from the theoretical calculations based on the two-dimensional spin-density wave scenario.[41] In addition, the log(T) divergence is also explained by the $Z=3$ quantum criticality of Fermi surface fluctuations of the Kondo breakdown scenario.[23]

As shown in Fig. 1, a finite range of nFL behavior with $\Delta\rho=AT$ down to 75 mK appears between the T_{Hall} and T^* crossover lines and the FL behavior is recovered for $H>100$ kOe.[8] Between the T^* and T_{FL} crossover lines the exponent of resistivity increases from 1 to 2 as magnetic field increases. Therefore, the wide range of nFL behavior is robust in YbAgGe, in contrast to the general expectation of the field-tuned QCP in HF metals of which the FL behavior is recovered when long range magnetic order is suppressed to zero temperature ($T_N \rightarrow 0$). On the other hand, particularly for $\Delta T \| \mathbf{c}$, the TEP is proportional to the temperature below T^* crossover line. The constant α corresponding to a saturation of $S(T)/T$ is seen at least up to 1 K for $H=90$ kOe and up to ~4 K for 140 kOe [Fig. 9(b)]. The observed large value of α in the zero temperature limit is characteristic of the HF state. The range with constant α is enlarged upon increasing field and the absolute value of α decreases, in agreement with the results of $C(T)/T$.[6,9] Based on the constant α, reflecting the FL region, the crossover temperature (T_{FL}) from nFL to FL obtained from TEP does not coincide with the one determined from resistivity measurements.[8] From the TEP results for $\Delta T \| \mathbf{c}$, AFM order and the FL state are not directly connected by a QCP but are separated by the domelike region IV. In order to clearly address this discrepancy between resistivity and TEP results as well as the anisotropic TEP response for different heat-current directions, it is necessary to measure TEP with magnetic field higher than 90 kOe and temperature down to millikelvin range. Note that $S(T)/T$ for $\Delta T \| \mathbf{ab}$ is continuously suppressed for $H>70$ kOe, indicating a tendency of saturation of α.

Up to this point several qualitative correlations between TEP and specific heat have been mentioned. More quantitatively, many HF compounds have shown correlations between $C(T)/T$ and $S(T)/T$ in the zero temperature limit, linking these two quantities via the dimensionless ratio $q=\frac{SN_Ae}{\gamma T} \sim \pm 1$, where N_A is the Avogadro number and the constant N_Ae is called the Faraday number.[42] Within the framework of the FL picture, both TEP and specific heat are linearly proportional to temperature, leading to the low-temperature saturation of $S(T)/T=\alpha$ and $C(T)/T=\gamma$. Fundamentally, this correlation can be linked to entropy considerations because the entropy is carried by the heat current due to temperature and electric potential gradients. It should be noticed that the relation, $q=\pm 1$, was derived for a single-band FL, therefore in a multi-band system, one should consider the contributions to q from all bands. Here, as proposed in Ref. 43, we have assumed the contribution of $S(T)$ from the heavier band dominates in YbAgGe.

Since we are currently limited to TEP data down to 0.35 K, we compare $C(T)/T$ to $S(T)/T$ at $T=0.4$ K. As shown in Fig. 10(a), although $S(T)/T$ data (left axis) show somewhat different magnetic field dependence between $\Delta T \| \mathbf{ab}$ and $\Delta T \| \mathbf{c}$, especially for $H<45$ kOe, the $S(T)/T$ data sets at $T=0.4$ K are fundamentally similar. $C(T)/T$ data (right axis) at 0.39 K are taken from the Ref. 9. Figure 10(b) presents q value as a function of magnetic field. In the vicinity of H_c ~45 kOe, q is much less than unity ($q \rightarrow 0$) for both ΔT

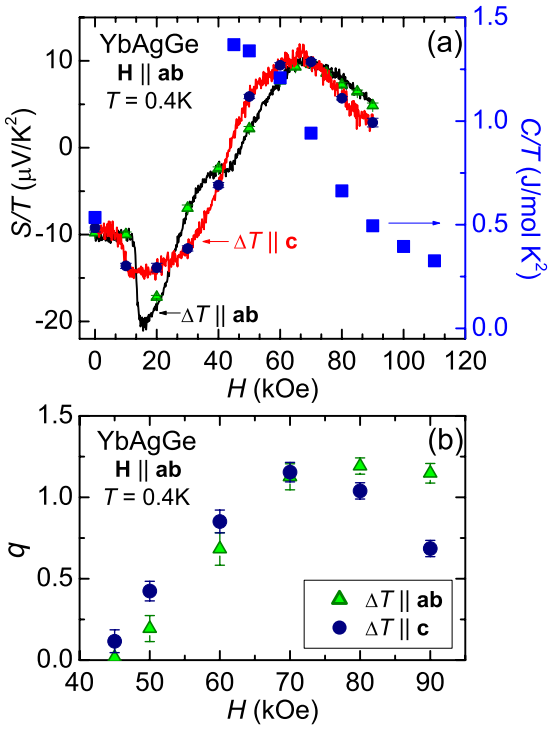

FIG. 10. (Color online) (a) $S(H)/T$ of YbAgGe at $T=0.4$ K for both $\Delta T \| \mathbf{ab}$ and $\Delta T \| \mathbf{c}$, plotted as a function of magnetic field, applied along $\mathbf{H} \| \mathbf{ab}$ in a transverse configuration ($\mathbf{H} \perp \Delta T$). Solid symbols (triangles and circles) are taken from temperature sweeps $S(T)/T$. Sommerfeld coefficient ($C(T)/T$, right axis) at 0.39 K was taken from the previous specific heat measurements (Ref. 9). (b) The estimated q values at $T=0.4$ K for both $\Delta T \| \mathbf{ab}$ and $\Delta T \| \mathbf{c}$, plotted as a function of H.

directions. Basically the small q value near H_c is due to the small value of α, where the sign of TEP changes from negative to positive. As magnetic field increases, the q value increases inside the domelike region, and then reaches order of unity at 70 kOe for both ΔT directions. For $H>70$ kOe q value for $\Delta T \| \mathbf{ab}$ remains close to the order of unity whereas q value for $\Delta T \| \mathbf{c}$ decreases as magnetic field increases. The separation of q values is due to $S(H)/T$ data heading back toward to zero, amplifying of a relatively small difference between the $\Delta T \| \mathbf{ab}$ and $\Delta T \| \mathbf{c}$ data. For comparison with $YbRh_2Si_2$,[16] it has been observed that the sign of q changes from positive to negative near the QCP; $q>0$ for $H<H_c$ and $q<0$ for $H>H_c$. The $S(T)/T$ value of $YbRh_2Si_2$ in the zero temperature limit does not scaled well with γ ($q \neq 1$) in the paramagnetic state. A recent theoretical investigation of the ratio q shows that q decreases considerably toward AFM-QCP but does not change significantly for a ferrromagnetic-QCP.[43] At this stage, we cannot offer a decisive comparison between theoretical work and our results because the ratio q is compared at finite temperature of $T=0.4$ K and manifests an anisotropic response for different ΔT directions; both further theoretical investigations and experimental measurements down to sub-millikelvin range are needed. Based on our results, one should notice that the observed sign of q is negative in zero field and positive for $H>H_c$ due to the sign of TEP. In zero field it has been shown that the sign of q is positive for Ce-based compounds and negative for Yb-based compounds.[42] In the presence of the magnetic field the observed sign of q for YbAgGe does not follow the general trend, thus further investigations including theoretical work are needed to clarify the discrepancy.

V. SUMMARY AND CONCLUSIONS

TEP data on YbAgGe have been collected down to $T \sim 0.3$ K and applied magnetic fields up to 140 kOe for $\mathbf{H} \| \mathbf{ab}$ and $\Delta T \| \mathbf{ab}$ as well as $\Delta T \| \mathbf{c}$. In zero field, the TEP data reveal characteristic features of a local minimum ($T_{\min}=85$ K), local maximum ($T_{\max}=15$ K), and an abrupt jump below 1 K, which correspond to the CEF level splitting (Δ_{CEF}), Kondo temperature (T_K), and long range magnetic order, respectively, as relevant energy scales in YbAgGe. The TEP response at the magnetic phase transition is anisotropic for the heat-current direction between in the hexagonal **ab** plane and along the **c** axis. The TEP measurements reproduce the earlier H-T phase diagram and identify an additional domelike phase between $\sim$45 and $\sim$70 kOe, associated with anomalous, $\rho(T) \propto T$, resistivity. Two characteristic crossover lines, constructed mostly from earlier Hall resistivity, are confirmed, clarified, and extended to higher temperature from the TEP results. These crossover lines show a tendency of converging toward to $H_c \sim 45$ kOe and $H^* \sim 70$ kOe in the zero temperature limit. The temperature and magnetic field range of nFL behavior ($\Delta\rho \propto T$) observed in resistivity are well matched with the domelike area in the phase diagram. For $H=70$ kOe data, adjacent to the domelike area, $S(T)/T$ for $\Delta T \| \mathbf{c}$ exhibits clearly a logarithmic temperature dependence in agreement with earlier specific heat results $C(T)/T \propto -\log(T)$. The present TEP results, combined with earlier specific heat and resistivity results, show a strong evidence of quantum critical fluctuations around $H \simeq 70$ kOe. The ratio of q, reflecting the correlations between $S(T)/T$ and $C(T)/T$, is much less than unity ($q \to 0$) in the vicinity of the $H_c \simeq 45$ kOe. As magnetic field increases from H_c the q value is recovered an order of unity at $H^* \simeq 70$ kOe. For $H>70$ kOe the enhanced value of $S(T)/T$ is indicative of the heavy fermion state, supporting previous specific heat and resistivity results.

ACKNOWLEDGMENTS

We would like to acknowledge G. M. Schmiedeshoff for useful discussions. We also acknowledge our former group members, Y. Janssen and E. Morosan, for previous sample growths. Work at Ames Laboratory was supported by the Basic Energy Sciences, U.S. Department of Energy under Contract No. DE-AC02-07CH11358.

[1] P. Gegenwart, Q. Si, and F. Steglich, Nat. Phys. **4**, 186 (2008).
[2] See, for example, G. R. Stewart, Rev. Mod. Phys. **73**, 797 (2001); **78**, 743 (2006).
[3] H. v. Löhneysen, T. Pietrus, G. Portisch, H. G. Schlager, A. Schröder, M. Sieck, and T. Trappmann, Phys. Rev. Lett. **72**, 3262 (1994).
[4] N. D. Mathur, F. M. Grosche, S. R. Julian, I. R. Walker, D. M. Freye, R. K. W. Haselwimmer, and G. G. Lonzarich, Nature (London) **394**, 39 (1998).
[5] O. Trovarelli, C. Geibel, S. Mederle, C. Langhammer, F. M. Grosche, P. Gegenwart, M. Lang, G. Sparn, and F. Steglich, Phys. Rev. Lett. **85**, 626 (2000).
[6] S. L. Bud'ko, E. Morosan, and P. C. Canfield, Phys. Rev. B **69**, 014415 (2004).
[7] K. Katoh, Y. Mano, K. Nakano, G. Terui, Y. Niide, and A. Ochiai, J. Magn. Magn. Mater. **268**, 212 (2004).
[8] P. G. Niklowitz, G. Knebel, J. Flouquet, S. L. Bud'ko, and P. C. Canfield, Phys. Rev. B **73**, 125101 (2006).
[9] Y. Tokiwa, A. Pikul, P. Gegenwart, F. Steglich, S. L. Bud'ko, and P. C. Canfield, Phys. Rev. B **73**, 094435 (2006).
[10] S. L. Bud'ko, E. Morosan, and P. C. Canfield, Phys. Rev. B **71**, 054408 (2005).
[11] S. L. Bud'ko, V. Zapf, E. Morosan, and P. C. Canfield, Phys. Rev. B **72**, 172413 (2005).
[12] K. Umeo, K. Yamane, Y. Muro, K. Katoh, Y. Niide, A. Ochiai, T. Morie, T. Sakakibara, and T. Takabatake, J. Phys. Soc. Jpn. **73**, 537 (2004).
[13] B. Fåk, D. F. McMorrow, P. G. Niklowitz, S. Raymond, E. Ressouche, J. Flouquet, P. C. Canfield, S. L. Bud'ko, Y. Janssen, and M. J. Gutmann, J. Phys.: Condens. Matter **17**, 301 (2005).
[14] B. Fåk, Ch. Rüegg, P. G. Niklowitz, D. F. McMorrow, P. C. Canfield, S. L. Bud'ko, Y. Janssen, and K. Habicht, Physica B **378-380**, 669 (2006).
[15] D. F. McMorrow *et al.*, Proceedings of the 25th International Conference on Low Temperature Physics, Amsterdam 2008 (unpublished).
[16] S. Hartmann, N. Oeschler, C. Krellner, C. Geibel, S. Paschen, and F. Steglich, Phys. Rev. Lett. **104**, 096401 (2010).
[17] K. Izawa, K. Behnia, Y. Matsuda, H. Shishido, R. Settai, Y. Onuki, and J. Flouquet, Phys. Rev. Lett. **99**, 147005 (2007).
[18] E. Morosan, S. L. Bud'ko, P. C. Canfield, M. S. Torikachvili, and A. H. Lacerda, J. Magn. Magn. Mater. **277**, 298 (2004).
[19] E. Mun, S. L. Bud'ko, M. S. Torikachvili, and P. C. Canfield, Meas. Sci. Technol. **21**, 055104 (2010).
[20] U. Köhler, N. Oeschler, F. Steglich, S. Maquilon, and Z. Fisk, Phys. Rev. B **77**, 104412 (2008).
[21] G. Aeppli, H. Yoshizawa, Y. Endoh, E. Bucher, J. Hufnagl, Y. Onuki, and T. Komatsubara, Phys. Rev. Lett. **57**, 122 (1986).
[22] J. Sakurai, A. Iwasaki, Q. Lu, D. Huo, Y. Isikawa, J. R. Fernández, and J. C. Gómez Sal, J. Phys. Soc. Jpn. **71**, 2829 (2002).
[23] K.-S. Kim and C. Pépin, Phys. Rev. B **81**, 205108 (2010).
[24] F. J. Blatt, P. A. Schroeder, C. Foiles, and D. Greig, *Thermoelectric Power of Metals* (Plenum, New York, 1976).
[25] J. M. Ziman, *Electrons and Phonons* (Oxford University Press, Oxford, England, 1960).
[26] A. K. Bhattacharjee and B. Coqblin, Phys. Rev. B **13**, 3441 (1976).
[27] Y. Lassailly, A. K. Bhattacharjee, and B. Coqblin, Phys. Rev. B **31**, 7424 (1985).
[28] K. Alami-Yadri, D. Jaccard, and D. Andreica, J. Low Temp. Phys. **114**, 135 (1999).
[29] V. Zlatić and R. Monnier, Phys. Rev. B **71**, 165109 (2005).
[30] T. Matsumura, H. Ishida, T. J. Sato, K. Katoh, Y. Niide, and A. Ochiai, J. Phys. Soc. Jpn. **73**, 2967 (2004).
[31] R. J. Elliott, *Magnetic Properties of Rare Earth Metals* (Plenum, London, 1972).
[32] S. Maekawa, S. Kashiba, M. Tachiki, and S. Takahashi, J. Phys. Soc. Jpn. **55**, 3194 (1986).
[33] N. E. Bickers, D. L. Cox, and J. W. Wilkins, Phys. Rev. B **36**, 2036 (1987).
[34] M. Očko, J. L. Sarrao, and Ž. Šimek, J. Magn. Magn. Mater. **284**, 43 (2004).
[35] Y. Aoki, T. D. Matsuda, H. Sugawara, H. Sato, H. Ohkuni, R. Settai, Y. Ōnuki, E. Yamamoto, Y. Haga, A. V. Andreev, V. Sechovsky, L. Havela, H. Ikeda, and K. Miyake, J. Magn. Magn. Mater. **177-181**, 271 (1998).
[36] G. M. Schmiedeshoff (private communication).
[37] H. Kubo, K. Umeo, K. Katoh, A. Ochiai, and T. Takabatake, J. Phys. Soc. Jpn. **79**, 064715 (2010).
[38] S. Friedemann, T. Westerkamp, M. Brando, N. Oeschler, S. Wirth, P. Gegenwart, C. Krellner, C. Geibel, and F. Steglich, Nat. Phys. **5**, 465 (2009).
[39] J. Custers, P. Gegenwart, C. Geibel, F. Steglich, P. Coleman, and S. Paschen, Phys. Rev. Lett. **104**, 186402 (2010).
[40] J. Benz, C. Pfleiderer, O. Stockert, and H. v. Löhneysen, Physica B **259-261**, 380 (1999).
[41] I. Paul and G. Kotliar, Phys. Rev. B **64**, 184414 (2001).
[42] K. Behnia, D. Jaccard, and J. Flouquet, J. Phys.: Condens. Matter **16**, 5187 (2004).
[43] K. Miyake and H. Kohno, J. Phys. Soc. Jpn. **74**, 254 (2005).